Non-Resonant Surface-Micromachined Z-Axis Gyroscopes Utilizing Torsional Out-of-Plane Detection

Cenk Acar
Microsystems Laboratory
University of California, Irvine
Irvine, CA, USA
cacar@uci.edu

Andrei M. Shkel
Microsystems Laboratory
University of California, Irvine
Irvine, CA, USA
ashkel@uci.edu

Abstract

This paper reports a novel gimbal-type torsional z-axis micromachined gyroscope with a non-resonant actuation scheme. The design concept is based on employing a 2 degrees-of-freedom (2-DOF) drive-mode oscillator to achieve dynamical amplification of oscillations, and a flat region in the frequency response. By utilizing dynamic amplification of torsional oscillations in the drive-mode instead of resonance, large oscillation amplitudes of the sensing element is achieved with small actuation amplitudes, providing improved linearity and stability despite parallel-plate actuation. With the flat region in the frequency response, the drive direction amplitude and phase are inherently constant within the same frequency band, while the device operates at resonance in the sense direction for improved sensitivity. Thus, the design concept is expected to overcome the small actuation and sensing capacitance limitation of surface-micromachined gyroscopes, while achieving improved excitation stability and robustness against fabrication imperfections and fluctuations in operation conditions.

Keywords

MEMS, Inertial Sensors, Micromachined Gyroscopes.

INTRODUCTION

Batch-fabrication of micromachined gyroscopes in VLSI compatible surface-micromachining technologies constitutes the key factor in low-cost production and commercialization. Torsional structures allowing large actuation and detection capacitances in surface micromachining technologies have been reported for resonant x and y-axis gyroscopes [2]. However, the nominal capacitance of surface-micromachined z-axis gyroscopes, which are generally driven and sensed in-plane, are limited by the small thickness of the structural layer.

Micromachined z-axis gyroscopes that employ out-of-plane actuation and detection have been proposed in the literature, with large capacitive electrode plates [3]. However, highly non-linear and unstable nature of parallel-plate actuation limits the actuation amplitude of the gyroscope. In this paper, we propose a novel surface-micromachined torsional gyroscope design utilizing dynamical amplification of rotational oscillations to achieve large oscillation amplitudes about the drive axis without resonance; thus addressing the issues of electrostatic instability while providing large actuation and detection capacitances.

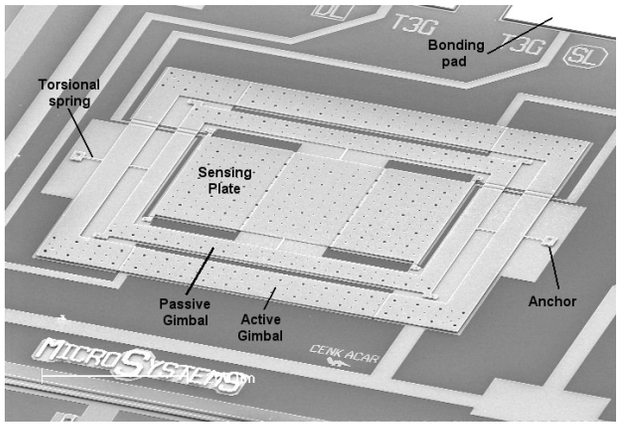

Figure 1. SEM micrograph of the fabricated prototype torsional micromachined gyroscopes.

THE TORSIONAL GYROSCOPE STRUCTURE

The overall torsional gyroscope system is composed of three interconnected rotary masses: the active gimbal, the passive gimbal, and the sensing plate (Figure 1). The active gimbal and the passive gimbal are free to oscillate only about the drive axis x. The sensing plate oscillates together with the passive gimbal about the drive axis, but is free to oscillate independently about the sense axis y, which is the axis of response when a rotation along z-axis is applied.

The active gimbal is driven about the x-axis by parallel-plate actuators formed by the electrode plates underneath. The combination of the passive gimbal and the sensing plate comprises the vibration absorber of the driven gimbal. Thus, a torsional 2-DOF oscillator is formed in the drive direction. With proper selection of parameters, large oscillation amplitudes in the passive gimbal, which contains the sensing plate, are achieved by amplifying the small oscillation amplitude of the driven gimbal (active gimbal). Thus, the actuation range of the parallel-plate actuators attached to the active gimbal is narrow, minimizing the nonlinear force profile and instability.

The sensing plate, which is the only mass free to oscillate about the sense axis, forms the 1-DOF torsional resonator in the sense direction. In the presence of an input angular rate about the sensitive axis normal to the substrate (z-axis), only

the sensing plate responds to the rotation-induced Coriolis torque. The oscillations of the sense plate about the sense axis are detected by the electrodes placed underneath.

The Coriolis Response

The design concept is based on operating at the sense-direction resonance frequency of the 1-DOF sensing plate, in order to attain the maximum possible oscillation amplitudes in response to the induced Coriolis torque. The frequency response of the 2-DOF drive direction oscillator has two resonant peaks and a flat region between the peaks (Figure 2). When the active gimbal is excited in the flat frequency band, amplitudes of the drive-direction oscillations are insensitive to parameter variations due to any possible fluctuation in operation conditions of the device.

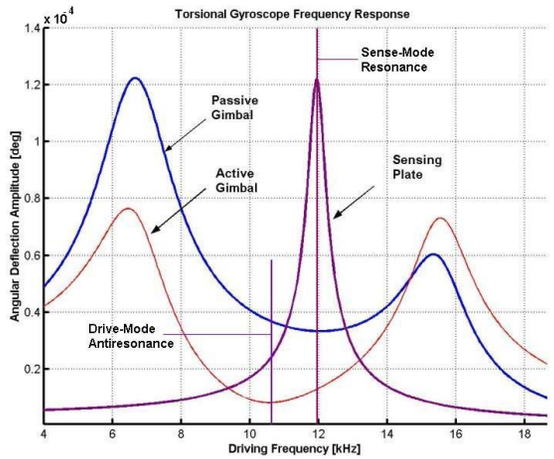

Figure 2. The frequency responses of the 2-DOF drive and 1-DOF sense-mode oscillators. The drive-direction oscillation amplitude is insensitive to parameter variations and damping fluctuations in the flat operating region.

To define the operation frequency band of the system, sense direction resonance frequency of the sensing plate is designed to coincide with the flat region of the drive oscillator (Figure 2). This allows operation at resonance in the sense direction for improved sensitivity, while the drive direction amplitude is inherently constant in the same frequency band, in spite of parameter variations or perturbations. Thus, the proposed design eliminates the mode-matching requirement by utilizing dynamic amplification of rotational oscillations instead of resonance in drive direction, leading to reduced sensitivity to structural and thermal parameter fluctuations and damping variations, while attaining sufficient performance with resonance in the sense-mode.

GYROSCOPE DYNAMICS

By attaching coordinate frames to the center-of-mass of each proof-mass and expressing the angular momentum equation for each mass in the non-inertial coordinate frames, the inertia matrix of each mass can be expressed in a diagonal and time-invariant form. Substitution of the angular velocity vectors into the angular momentum equations yields the dynamics of the sensing plate about the sense axis (y-axis), and the active and passive gimbal dynamics about the drive axis (x-axis). If we denote the drive direction deflection angle of the active gimbal with by θ_a, the drive direction deflection angle of the passive gimbal by θ_p, the sense direction deflection angle of the sensing plate by ϕ (with respect to the substrate), and the absolute angular velocity of the substrate about the z-axis by Ω_z; with the assumptions that the angular rate input is constant and the oscillation angels are small, the rotational equations of motion reduce to

$$I_y^s\ddot{\phi} + D_y^s\dot{\phi} + K_y^s\phi = (I_z^s + I_y^s - I_x^s)\dot{\theta}_p\Omega_z \quad (1)$$

$$(I_x^p + I_x^s)\ddot{\theta}_p + (D_x^p + D_x^s)\dot{\theta}_p + K_x^p\theta_p = K_x^p\theta_a \quad (2)$$

$$I_x^a\ddot{\theta}_a + D_x^a\dot{\theta}_a + K_x^a\theta_a = K_x^p(\theta_p - \theta_a) + M_d \quad (3)$$

where I^s, I^p, and I^a denote the moments of inertia of the sensing plate, the passive gimbal, and the active gimbal, respectively. D_x^s, D_x^p, and D_x^a are the drive-direction damping ratios, and D_y^s is the sense-direction damping ratio of the sensing plate; K_y^s is the torsional stiffness of the suspension beam connecting the sensing plate to the passive gimbal, K_x^p is the torsional stiffness of the suspension beam connecting the passive gimbal to the active gimbal, and K_x^a is the torsional stiffness of the suspension beam connecting the active gimbal to the substrate.

Torsional Suspension Members

The suspension system of the device that supports the gimbals and the sensing plate is composed of thin polysilicon beams with rectangular cross-section functioning as torsional bars. Assuming each torsional beam is straight with a uniform cross-section, and the structural material is homogeneous and isotropic; the torsional stiffness of each beam with a length of L can be modeled as [5]

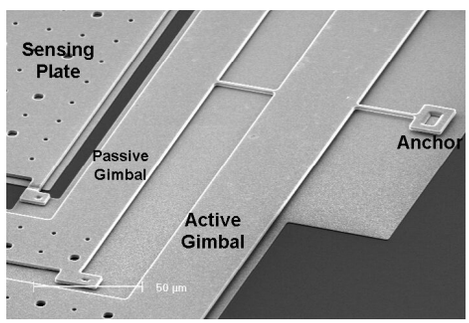

Figure 3. SEM micrograph of the torsional suspension beams in the prototype gyroscopes.

$$K = \frac{SG + \sigma J}{L} \quad (4)$$

where $G = \frac{E}{2(1-\nu)}$ is the shear modulus with the elastic modulus E and Poisson's ratio ν; σ is the residual stress; and $J = \frac{1}{12}(wt^3 + tw^3)$ is the polar moment of inertia

of the rectangular beam cross-section with a thickness of t and a width of w. The cross-sectional coefficient S can be expressed for the same rectangular cross-section as [5]

$$S = \left(\frac{t}{2}\right)^3 \frac{w}{2}\left[\frac{16}{3} - 3.36\frac{t}{w}\left(1 - \frac{t^4}{12w^4}\right)\right] \quad (5)$$

For the presented prototype design, the suspension beams lengths are $L_x^a = L_x^p = L_y^s = 30\mu$m, with the width of 2μm and a structural thickness of 2μm; resulting in the stiffness values of $K_x^a = K_x^p = K_y^s = 1.04 \times 10^{-18}$ kg m^2/s^2.

Finite Element Analysis Results

Theoretical analysis of the device geometry with a thickness of 2μm yields $(I_x^a + I_x^s) = 4.97 \times 10^{-18}$ kg m^2 and, $I_y^s = 4.94 \times 10^{-18}$kg m^2; resulting in $\omega_x^p = 7.285$kHz and $\omega_y = 7.263$kHz. Through FEA simulations, the sense mode resonance frequency of the sensing plate about the sense axis was obtained to be ω_y =7.457kHz, with a 2.28% discrepancy from the theoretical calculations. The drive-mode resonant frequency of the isolated passive mass-spring system was obtained as the first mode at ω_x^p =7.097kHz. The 5.91% discrepancy from theoretical analysis is attributed in part to the reduced stiffness due to the compliance of the active and passive gimbal frame structures.

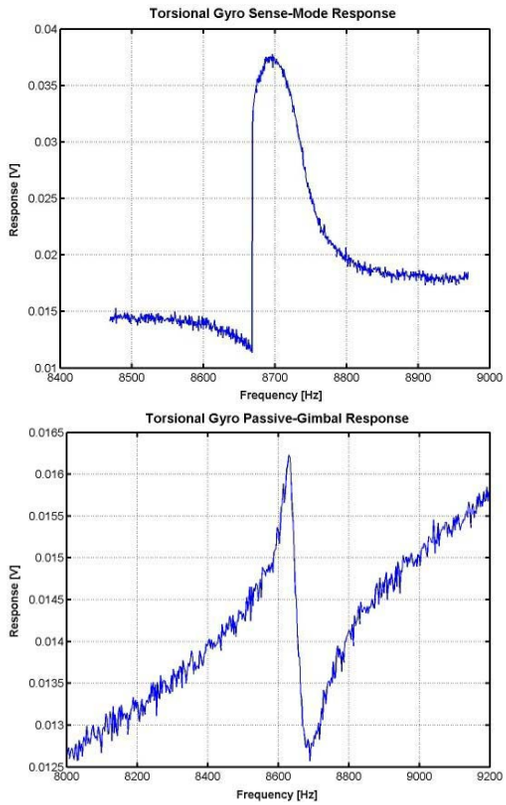

Figure 4. (Sense-mode and drive-mode frequency response acquired using off-chip transimpedance amplifiers, yielding ω_y= 8.725 kHz, and ω_x^p=8.687 kHz for 0.7V DC bias.

EXPERIMENTAL CHARACTERIZATION

The frequency response of the fabricated prototype gyroscope was acquired in an MMR Vacuum Probe Station using off-chip transimpedance amplifiers. Due to the large actuation and sensing capacitances, actuation voltages as low as 0.7V to 1.8V DC bias, and 30mV AC were used under 40mTorr vacuum. For detecting the drive-mode antiresonant frequency, which is equal to the resonant frequency of the isolated passive mass-spring system (ω_x^p), a separate test structure that consists of the passive gimbal-sensing plate assembly was used.

The resonance peaks in the sense and drive modes were observed very clearly for the 0.7V - 1.8V DC bias range. With a 0.7V DC bias, the sense-mode resonance frequency was measured to be 8.725 kHz (Figure 4a), and the drive-mode antiresonance frequency was measured to be 8.687 kHz (Figure 4b). The drive and sense mode resonance frequencies were electrostatically tuned by several hundred Hertz with only 1V DC bias tuning range (Figure 5). It was observed that ω_x^p and ω_y are exactly matched for $V_{dc} = 1.0$V.

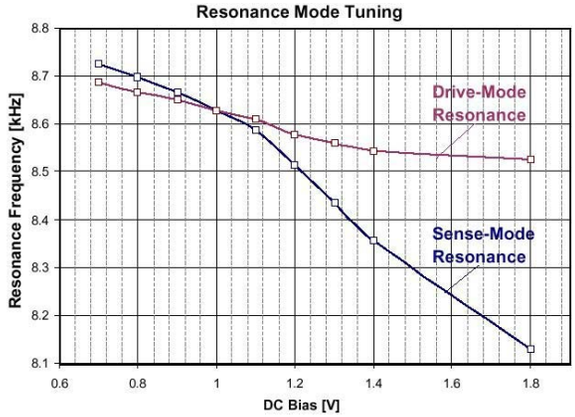

Figure 5. (a) Electrostatic tuning of the drive and sense mode resonance frequencies by changing the DC bias. Notice that ω_x^p and ω_y are exactly matched for $V_{dc} = 1.0$V.

To investigate the origins of the discrepancy between the measurements and FEA results, the prototype was analyzed using a PLμ Confocal Imaging Profiler, for obtaining the structural parameters, such as layer thickness, elevation, suspension beam geometry, and any possible curling in the structure (Figure 6). The structural layer thickness was measured as 1.97 μm, elevated by 2.1 μm from the substrate, with extremely small curling (10 nm elevation difference between the middle section and the edges). However, due to the corner rounding effects in photo-lithography, the effective length of the torsional suspension beams were observed as 27.1μm. When the FEA was repeated with the 27.1μm suspension length, the results agreed with experimental measurements to a great extent, with 3.6% discrepancy in the drive-mode, and 0.95% discrepancy in the sense-mode.

In order the verify the mode-shapes of the structure at the measured frequencies, a Polytec Scanning Laser Doppler

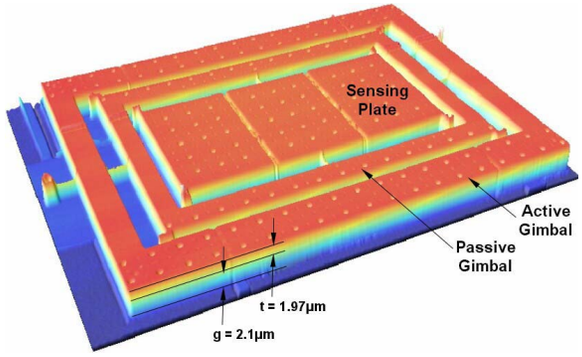

Figure 6. Confocal imaging profiler scan of the structure, for obtaining layer thickness, elevation, suspension beam geometry, and curling.

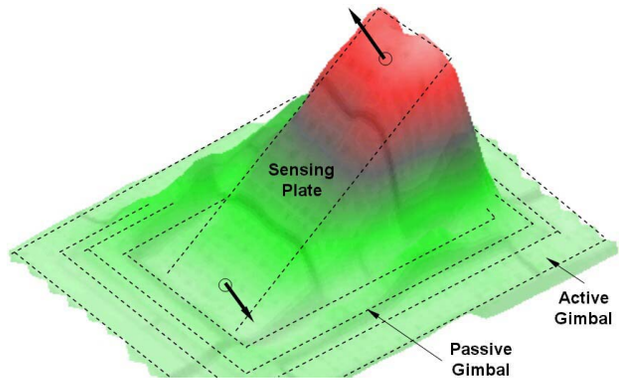

Figure 7. The sense-mode dynamic response measurements using the LDV in the scanning mode.

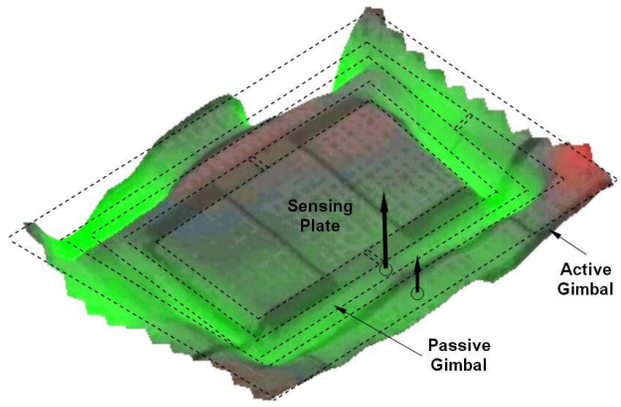

Figure 8. Scanning mode LDV measurements at the anti-resonance frequency, demonstrating dynamic amplification of the active gimbal oscillations by the passive gimbal. The passive gimbal was observed to achieve over 1.7 times larger oscillation amplitudes than the driven active gimbal.

Vibrometer was used in scanning mode under atmospheric pressure for dynamic optical profiling. Excitation of the sensing plate about the sense-axis at the experimentally measured sense-mode resonance frequency ($\omega_y = 8.725$ kHz) revealed that only the sensing plate responds in the sense mode, verifying that the 1-DOF resonator formed in the sense-mode is decoupled from the drive-mode (Figure 7), in agreement with the intended design and finite element analysis simulations. Dynamic excitation of the active gimbal about the drive-axis at frequencies away from the anti-resonance frequencies verified that the active gimbal oscillates independent from the passive gimbal-sensing plate assembly, constituting the active mass of the 2-DOF oscillator.

Most prominently, dynamic amplification of the active gimbal oscillations by the passive gimbal was successfully demonstrated. At the drive-mode anti-resonance frequency, which was measured to be 8.687 kHz, the passive gimbal was observed to achieve over 1.7 times larger oscillation amplitudes than the driven active gimbal (Figure 8). This translates into attaining over 2.4 times larger drive-mode deflection angles at the sensing plate than the active gimbal.

CONCLUSION

A novel torsional z-axis micromachined gyroscope with a non-resonant actuation scheme was presented, based on employing a 2-DOF drive-mode oscillator to achieve dynamical amplification of oscillations, and a flat region in the frequency response. Thus, the design concept allows to build surface-micromachined z-axis gyroscopes with large actuation and detection capacitances, while resulting in improved excitation stability and robustness against parameter fluctuations. With the operational principles experimentally verified, the approach is expected to relax control requirements and tight fabrication and packaging tolerances.

ACKNOWLEDGEMENTS

This work is supported in part by the National Science Foundation Grant CMS-0409923, program managers Dr. Shin-Chi Liu and Dr. Masayoshi Tomizuka.

REFERENCES

[1] C. Acar, and A. Shkel. Structural Design and Experimental Characterization of Torsional Micromachined Gyroscopes with Non-Resonant Drive-Mode. Journal of Micromechanics and Microengineering. Vol.14, pp.15-25, 2003.

[2] T.N. Juneau, A.P. Pisano, J.H. Smith. Dual Axis Operation of a Micromachined Rate Gyroscope. Ninth International Conference on Solid-State Sensors and Actuators, Chicago, IL, June 1997.

[3] S.E. Alper, and T. Akin. A Planar Gyroscope Using Standard Surface Micromachining Process. Conference on Solid-State Transducers, Copenhagen, Denmark, 2000, pp. 387-390.

[4] M. Niu, W. Xue, X. Wang, J. Xie, G. Yang, and W. Wang. Design and Characteristics of Two-Gimbals Micro-Gyroscopes Fabricated with Quasi-LIGA Process. International Conference on Solid-State Sensor and Actuators, 1997, pp. 891-894.

[5] W.C. Young. Roark's Formulas for Stress and Strain. McGraw-Hill, Inc., pp. 93-156, 1989.

[6] http://www.sensofar.com.

[7] http://www.polytecpi.com.